

Some Considerations on Strength and Ductility of RC Members with Low Strength Concrete

NEGUCHI Momoyo¹ and MINAMI Koichi²

¹ Graduate Student, Course of Regional Space Planning and Systems Engineering, Doctoral Program, Fukuyama University, Hiroshima, Japan

² Professor, Faculty of Engineering, Department of Architecture and Civil Engineering, Fukuyama University, Hiroshima, Japan

Email: neguchi@d3.dion.ne.jp, minami@fucc.fukuyama-u.ac.jp

ABSTRACT :

In this study, we experimented on 20 RC columns with low strength concrete (LSC) of 5, 10 and 15 N/mm² grade. The test specimens were experimented under constant compressive load and controlling the lateral displacement angle. The test specimens with round main reinforcements did not brake with shear failure due to very small bond stress of the main reinforcements, and a state of the shear compressive failure by the slippage compressive failure on the diagonal of the concrete appears conspicuously. Therefore, the relationship between shear load and the lateral displacement angle showed a property of ductility without the yield strength deterioration to 0.032 rad after maximum load although it almost showed the hysteresis curve of a remarkable reverse S-shaped. The maximum strength obtained from by a plasticity theory considering of a truss mechanism and an arch mechanism.

KEYWORDS: Low Strength Concrete, RC Members, Seismic Performance, Seismic Retrofit, Plastic Theory

1. INTRODUCTION

Seismic diagnosis and seismic retrofit of the existing buildings are performed nationwide in Japan. The seismic diagnosis revealed that there were many buildings of the low strength concrete (LSC) less than 13.5 N/mm² were found. That becomes the social problem how seismic performances for the buildings were secured with seismic retrofit. However, each the evaluation organization racks its brains about the correspondence because there are few studies about LSC. Seismic diagnosis method and the seismic retrofit technique for LSC are demanded socially by such present conditions. Table 1 shows concrete compressive strength of school building in a prefecture. Although this figure shows limited area in Japan, it is a problem that such buildings of concrete compressive strength less than 12 N/mm² exist, in spite of 12 N/mm² as lowest concrete compressive strength in Japanese Building Standard Act.

Seismic Evaluation Standard for Existing Reinforced Concrete Structure published from The Japan Building Disaster Prevention Association establishes the concrete compressive strength of buildings is applied to 13.5 N/mm² or more.[1] The one of the reasons is that there are not enough studies although some experimental studies have been made on LSC. Therefore, the performance of members of the LSC is not clear. [2]-[6]

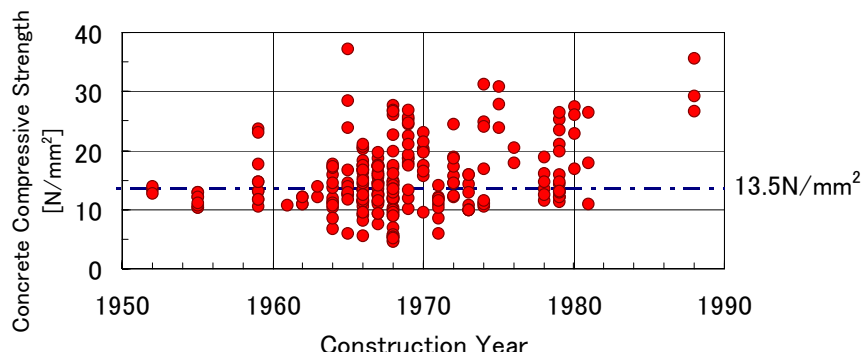


Fig. 1. Distribution of Concrete Compressive Strength

2. OUTLINE OF TESTS

The total number of 20 test specimens divided into 4 groups as Table 1, 16 test specimens are non-retrofit columns and 4 test specimens are retrofitted columns by carbon fiber sheets. The experimental parameters but

Table 1. Outline of Tests

Group No.	Column No.	Name of Specimens	Concrete Compressive Strength, σ_B	Longitudinal Reinforcement	Shear Reinforcement Ratio, p_w [%]	Axial Force Ratio $N/(bD \cdot \sigma_B)$	Layer of Carbon Fiber Sheets
I	1	L05200	3.7	16φ	0.21	0	none
	2	L05220				0.2	
	3	L05240				0.4	
	4	L05400			0.42	0	
	5	L05420				0.2	
	6	L05440				0.4	
II	7	L10200	12.3	16φ	0.21	0	none
	8	L10240				0.4	
	9	L10400			0.42	0	
	10	L10440		D16		0.4	
	11	DL10200		0.21	0		
	12	DL10240			0.4		
III	13	L1024C1	9.4	16φ	0.21	0.5 layer	none
	14	L1024C2				2 layer	
	15	DL1024C1		D16	0.4	0.5 layer	
	16	DL1024C2				2 layer	
IV	17	L15200	13.9	16φ	0.21	0	none
	18	L15240				0.4	
	19	L15400		D16	0.42	0	
	20	L15440				0.4	

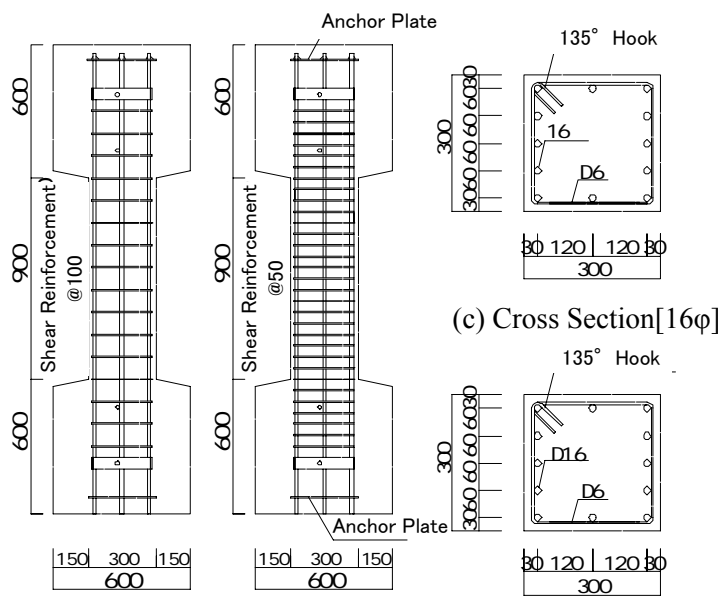


Fig. 2. Test Specimens [unit: mm]

Table 2. Concrete Mixture [kg/m^3]

Group No.	I	II, III	IV
Specified Design Strength	5	10	15
Water	210	210	210
Cement	90	148	188
CaCO_3	233	175	136
Fine Aggregate 1	501	506	509
Fine Aggregate 2	348	351	353
Coarse Aggregate 1	513	513	543
Coarse Aggregate 2	340	350	340
Air Entraining Agent	2.58	2.58	2.58

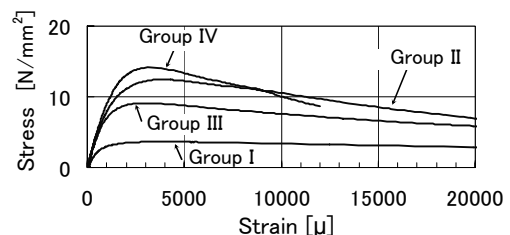


Fig. 3. Stress-Strain Relations for Concrete

concrete compressive strength are kinds of longitudinal reinforcements, shear reinforcement ratio, axial force ratio and layer of carbon fiber sheets. Most of parameters are chosen to compare with other test results of columns with normal compressive strength at Dr. MINAMI Laboratory.

Fig. 2 shows vertical and cross section of non-retrofit specimens, one of the notable features of this study is experimenting columns with not only deformed bars as longitudinal reinforcement but also round bars because the school buildings of LSC before 1965 have used round bars as longitudinal reinforcement. Deformed bars (D6) are used as shear reinforcement of all columns so that round bars (6ϕ) were unavailable.

The stress-strain relations for concrete by concrete mixture in Table 2 appear in Fig. 3. Each curve in Fig. 3 is the relation of the first test specimen in each group.

The loading rule experimented on by 0.2×10^{-2} rad by the same displacement amplitude to 3.2×10^{-2} rad twice.

3. TEST RESULTS

3.1. Final Failure Situation

Some photos of final failure situation of test specimens are shown in Photo. 1. The test specimen in (a), (b), (c) and (e) is used round bars as longitudinal reinforcement, in (d) and (f) is used deformed bars. The test specimens in Photo. 1 (a)-(d) are non-retrofit columns and (e) and (f) are retrofitted columns which winded up carbon fiber sheets.

The shear cracking width did not grow up in final displacement amplitude although the test specimens with round bars occurred to shear cracking, the test specimens finally collapsed by shear compressive failure with crashing of concrete of the end.

The test specimens with deformed bars occurred to shear cracking at central part and shear bond splitting cracking along longitudinal reinforcement, the test specimens finally collapsed by shear bond splitting failure with concrete flaking away.

The failure of the test specimens with round bars is different from that with deformed bars.

The retrofitted test specimen with round bars in Photo. 1 (e) hardly changed on surface until the last displacement amplitude, and which with deformed bars in Photo. 1 (d) gathered on carbon fiber sheets and occurred cracking after attaining the maximum strength. It was the notable feature of this test specimen with deformed bars and carbon fiber sheets of 0.5 layer that the cracking grew on carbon fiber sheets then carbon fiber sheets exfoliated with inside concrete.

3.2. Hysteresis Curve

Each sub caption of hysteresis curve in Fig. 3 is same as that in Photo. 1, axial force ratio of all test specimens in Fig. 3 is 0.4.

3 columns in Fig. 3 (a)-(c) are non-retrofit and used round bars as longitudinal reinforcement, the difference of 3 is concrete compressive strength. It is the feature that the decreased strength after the maximum strength became big so that concrete compressive strength is high, however the ratio of decreased strength of columns with round bars is smaller than that with deformed bars in Fig. 3 (d).

Regardless of the kind of the longitudinal reinforcement, the decreased strength of the retrofitted columns tend not to occur than which of non-retrofit columns.

3.3. Envelope Curve

The axial force ration in Fig. 4 (a) is 0, in Fig. 4 (b) is 0.4, the difference is concrete compressive strength.

It is admitted that the maximum strength rises if concrete compressive strength becomes high, the test specimens of axial force ratio 0 hardly occurred the decreased strength until the last displacement amplitude, and the test specimens of axial force ratio 0.4 tended to become big decreased strength after attaining the maximum strength.

The retrofit effect was shown clearer to the column with deformed bars in Fig. 4 (c) than that with round bars in Fig. 4 (d). Then, it was found from the result that the decreased strength hardly occurred after the maximum strength when layer of carbon fiber sheets increased.

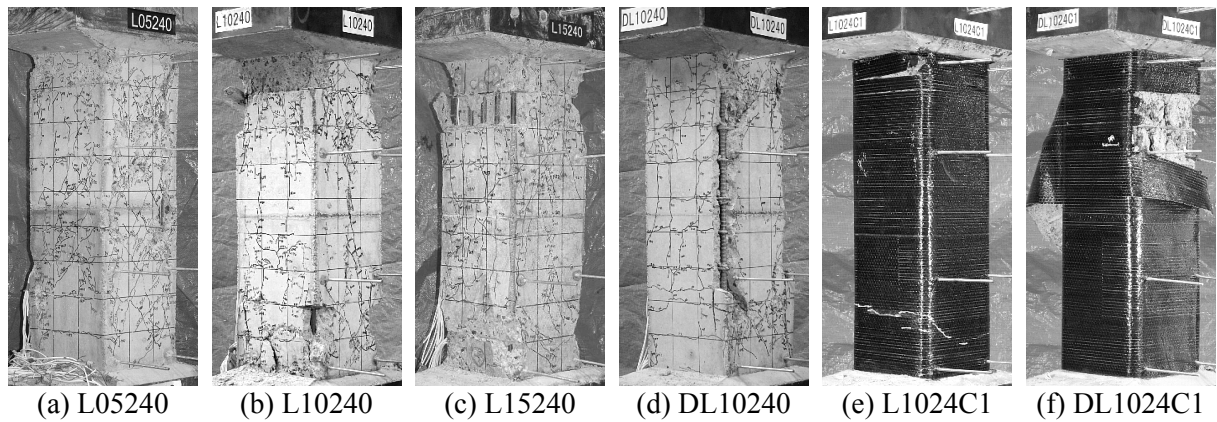


Photo. 1. Final Destruction Situation

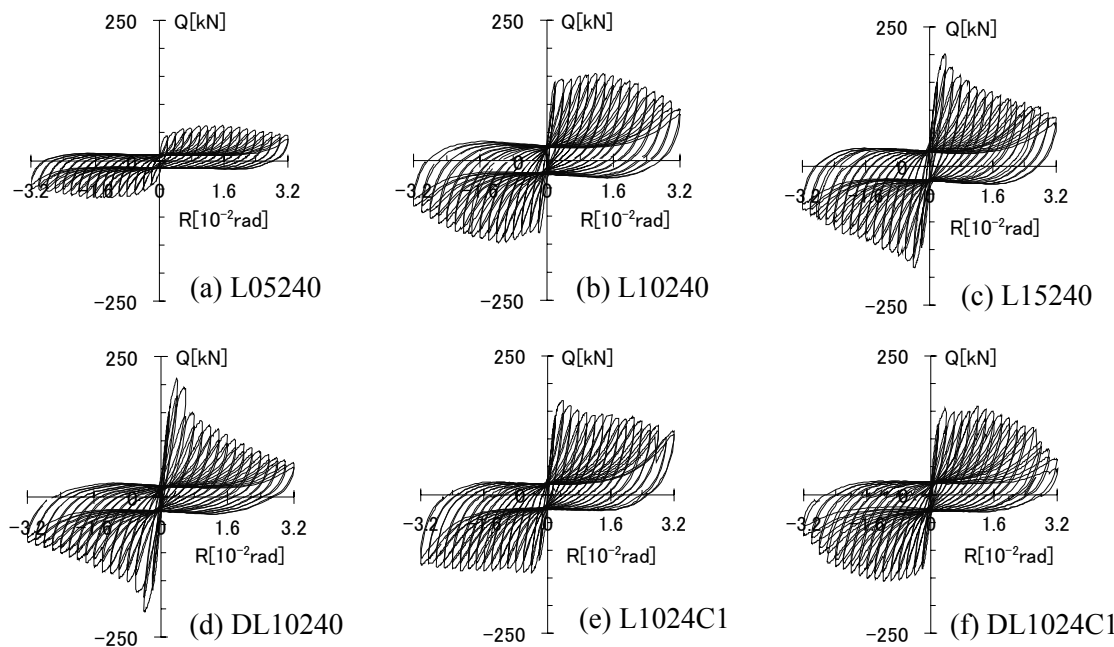


Fig. 4. Hysteresis Curve

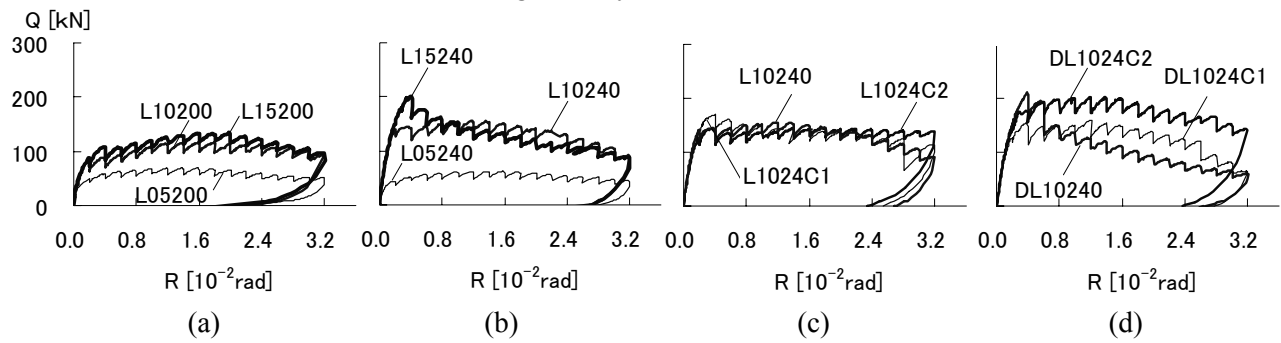


Fig. 5. Envelope Curve for Positive Loading

3.4. Tensile Stress on Shear Reinforcement

Fig. 6 shows that the mean of ξ_P and ξ_S , the measured tensile stress on shear reinforcement divided by the yield stress each P direction (an orthogonality direction of the action shear load) and S direction (a same direction of the action shear load), in displacement amplitude of 0.20×10^{-2} rad, 0.60×10^{-2} rad, 1.00×10^{-2} rad and the maximum loading. ξ_P tend to increase with increase of the displacement amplitude, column no. 11 takes the maximum ξ_P value of all columns, however to be the maximum is around 0.4, and the value is not a big value compared with studies of past. On the other hand, although the value of ξ_S is higher than the value of ξ_P , the all

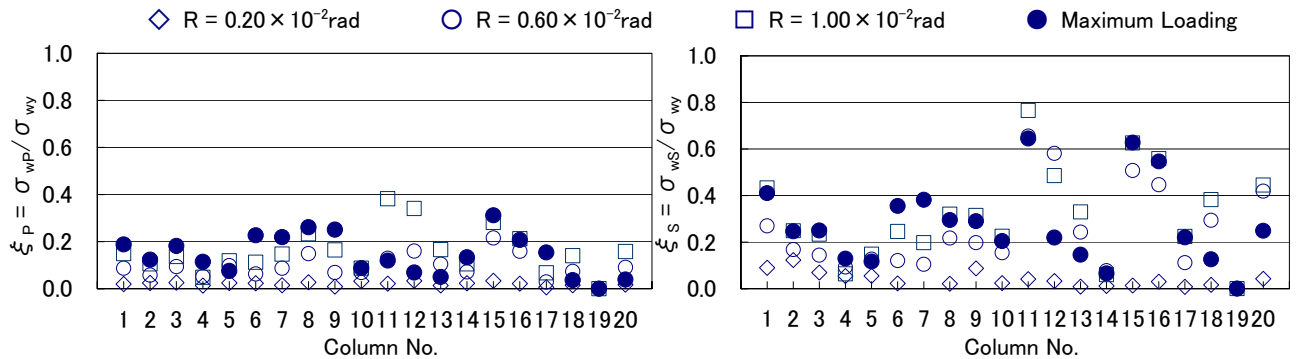


Fig. 6. Values of ξ_p and ξ_s Based on Tensile Stress of Shear Reinforcement

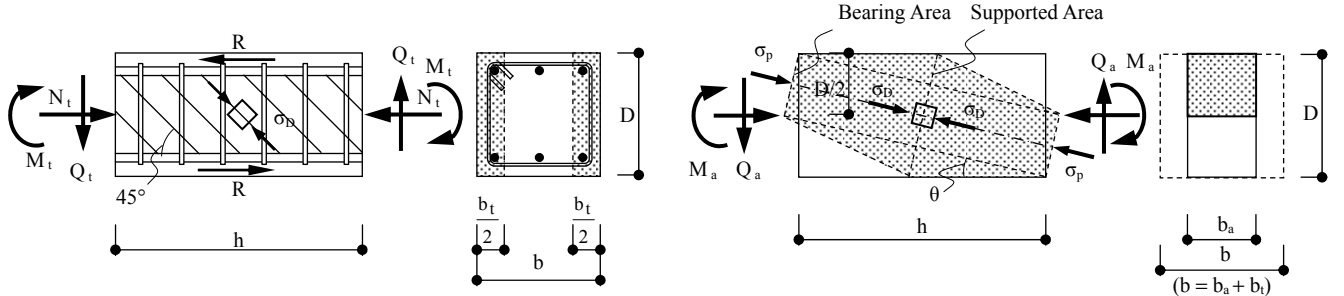


Fig. 7. Truss Mechanism with Bond Splitting Failure

Fig. 8. Arch Mechanism in Local Compressive Field

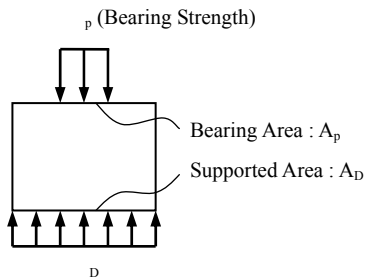


Fig. 9. Bearing Strength

$$\sigma_p = \sqrt{\frac{A_D}{A_p}} \cdot \sigma_0$$

$$\sigma_D \rightarrow \sigma_B$$

$$\sigma_p = \sqrt{\frac{A_D}{A_p}} \cdot \sigma_B \leq 2\sigma_B$$

shear reinforcements of columns did not yield. It is important that it should not presuppose that shear reinforcement yield in the evaluation of the ultimate strength.

4. EVALUATION BASED ON THE PLASTIC THEORY

We try the evaluation of the ultimate shear strength of the LSC columns based on Chapter 6 of *Design Guideline for Earthquake Resistant Reinforced Concrete Buildings Based on Ultimate Strength Concept* published in 1990. [10]

At first, the shear resistance mechanism is the model of allowing mixture of the truss mechanism and the arch mechanism, the strength of the truss mechanism is decided by the bond stress on longitudinal reinforcement. Assuming that the angle of inclination of the unyield shear reinforcement is 45° for transmitting the bond stress, the concrete compressive strength σ_B is kept in the concrete compressive field in Fig. 7. Then Q_{Ut} , the ultimate shear strength of the bond stress, is evaluated by Eq. (1).

$$Q_{Ut} = \tau_{Ub} \cdot \Sigma \varphi \cdot D \quad (1)$$

$$\text{where, } \tau_{Ub} = \frac{\varepsilon \cdot A \cdot E}{\ell \cdot \varphi} \quad (2)$$

ε : strain, A: area of longitudinal reinforcement[mm²],
E: Young's modulus, ℓ : bond splitting length[mm],
 ϕ : perimeter of longitudinal reinforcement[mm]

in addition, for establishing the mechanism, the width b_t of concrete compressive field is given by Eq. (3).

$$b_t = 2 \cdot \frac{\tau_{ub}}{\sigma_B} \cdot \Sigma \phi \quad (3)$$

It is assumed that the arch mechanism in Fig. 8 is constituted when the resultant uniaxial compressive stress, σ_o , of the normal stress, σ_p , both uniformly distributed over the compression region at both ends of the reinforcement-less concrete with the width b_a which is the remaining width used for the arch mechanism and given by Eq. (4), are produced in the direction that is off from the member axis by the angle of θ . Further, the maximum shear resistance of the arch mechanism is assumed to take place when the above-mentioned resultant stress, σ_o , reaches σ_B , when the shear strength, Q_{Ual} , can be expressed by Eq. (5).

$$b_a = b - b_t \quad (4)$$

$$Q_{Ual} = \left[\sqrt{4 + \left(\frac{\eta}{c n_0} \right)^2 - 4 c n_0^2} - \left(\frac{\eta}{c n_0} \right) \right] \cdot \frac{b_a \cdot D \cdot \sigma_B}{2} \quad (5)$$

where, $\eta = h/D$

$$c n_0 = \sqrt{\frac{\sqrt[3]{\eta^2 + \eta^2 \sqrt{1 + \eta^2}}}{2} + \frac{\sqrt[3]{\eta^2 - \eta^2 \sqrt{1 + \eta^2}}}{2}} \quad (6)$$

The Q_{su2} is given by superposition of Q_{Ut} and Q_{Ual} by Eq. (7).

$$Q_{su2} = Q_{Ut} + Q_{Ual} \quad (7)$$

Furthermore, the confined effective for concrete as ξ_p given by the measured tensile stress on shear reinforcement is evaluated by Eq. (8). [11]

$$\sigma_B' = \lambda \cdot \sigma_B \quad (8)$$

$$\text{where, } \lambda = 1 + 2.05 \frac{p_w \cdot \xi_p \cdot \sigma_{wy}}{\sigma_B} \quad (9)$$

Let σ_B' be σ_B in Eq. (5), the strength of the arch mechanism considered the confined effective for concrete is given by Eq. (10). [11] (Fig. 9)

$$Q_{Ua2} = \lambda \cdot Q_{Ual} \quad (10)$$

Then, the ultimate shear strength Q_{su3} is given by superposition Q_{Ut} and Q_{Ua2} by Eq. (11)

$$Q_{su3} = Q_{Ut} + Q_{Ua2} \quad (11)$$

The provided calculated results are shown in Table 3 and Fig. 10 by the above-mentioned equations. Assuming that the shear resistance mechanism is only arch mechanism, the calculated ultimate shear strength does not correspond to the experimental strength well. Especially, the ultimate shear strength of columns with deformed bars is evaluated lower than the experimental strength. Assuming that the shear resistance mechanism is the superposition of the arch mechanism and truss mechanism, the calculated ultimate shear

Table 3. Ultimate Shear Strength

Column No.	Name of Test Specimen	Experimental Strength		Calculated Strength Based on the Plastic Theory			λ
		Positive Load Q_{sU0} [kN]	Negative Load Q_{sU0} [kN]	Q_{sU1} [kN]	Q_{sU2} [kN]	Q_{sU3} [kN]	
1	L05200	69.0	-62.0	36.8	61.8	64.8	1.08
2	L05220	65.9	-69.0	37.5	63.0	65.0	1.05
3	L05240	65.4	-69.4	40.0	67.2	70.1	1.07
4	L05400	61.3	-58.5	32.1	54.0	57.6	1.11
5	L05420	74.2	-63.7	34.3	57.6	60.0	1.07
6	L05440	78.1	-74.8	35.0	58.8	66.0	1.19
7	L10200	117.6	-134.0	115.9	194.8	197.5	1.02
8	L10240	160.8	-154.0	119.9	201.4	204.4	1.02
9	L10400	144.1	-137.8	112.0	188.1	193.8	1.05
10	L10440	142.9	-138.8	116.6	195.9	197.9	1.02
11	DL10200	160.1	-161.2	121.2	220.3	221.5	1.01
12	DL10240	212.5	-206.6	123.2	223.3	224.1	1.01
13	L1024C1	171.4	-143.2	83.6	140.4	141.0	1.01
14	L1024C2	154.4	-141.4	84.7	142.4	143.9	1.02
15	DL1024C1	164.8	-161.6	86.5	169.2	172.3	1.04
16	DL1024C2	206.7	-206.1	88.3	181.9	183.9	1.02
17	L15200	135.9	-152.8	125.6	211.0	215.8	1.04
18	L15240	203.7	-185.7	119.1	200.1	200.7	1.00
19	L15400	144.5	-135.6	129.7	218.0	241.8	1.17
20	L15440	201.6	-183.7	120.3	202.1	203.4	1.01

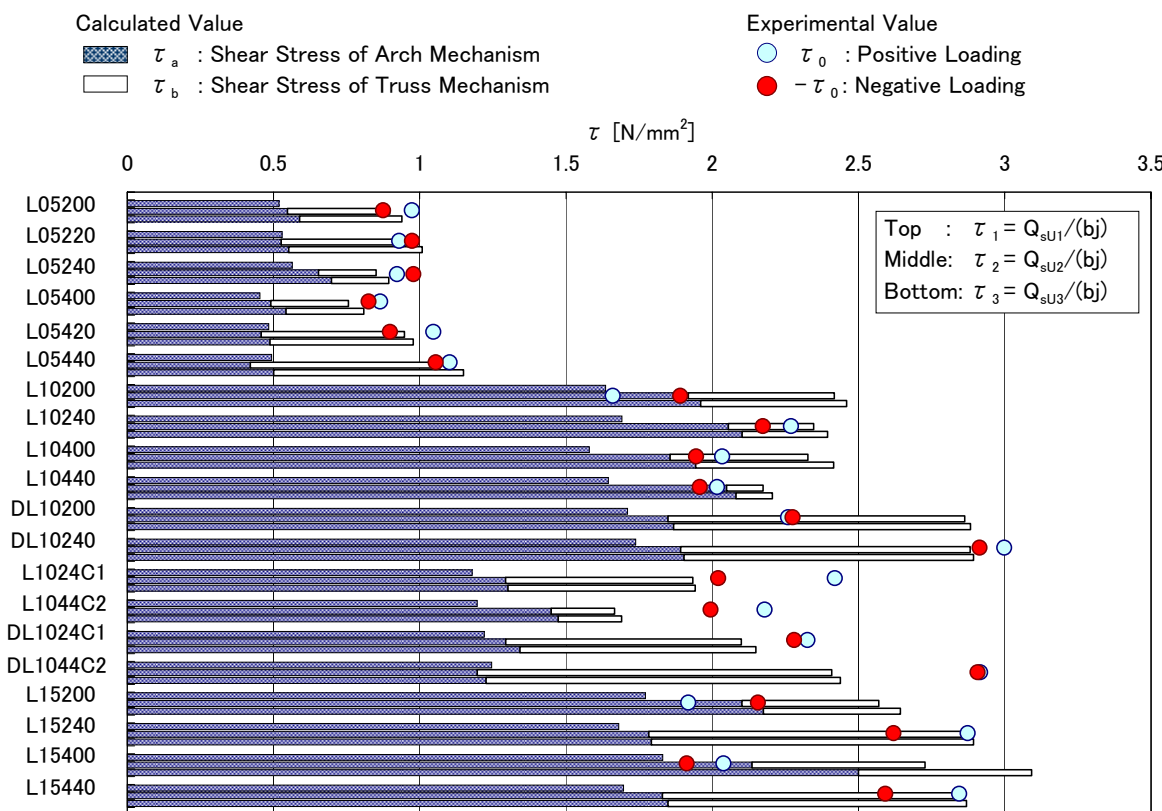


Fig. 10 Evaluation of Ultimate Stress by Plastic Theory

strength corresponds to the experimental strength. Then, the quantification of the confined effective for concrete by the shear reinforcement or carbon fiber sheets remains as a matter to be considered further.

5. CONCLUSION

The following results were obtained in this paper:

- (1) Even if the column with LSC of 5 N/mm^2 grade and round bars as longitudinal reinforcement, it was able to perform cyclic load to the displacement amplitude of 3.2×10^{-2} rad, did not finally occur the decreased strength.
- (2) The columns with round bars as longitudinal reinforcement finally failed by the shear compressive failure with crushing the end of concrete although the cracking did not grow.
- (3) The retrofit effect clearly appeared on the columns with deformed bars as longitudinal reinforcement.
- (4) The ultimate shear strength is able to evaluate by the plastic theory, however it is necessary to further examine the quantification of the confined effective.

REFERENCES

- [1] The Japan Building Disaster Prevention Association (2001). Seismic Evaluation Standard for Existing Reinforced Concrete Structure, (in Japanese)
- [2] Yamamoto, Y., Akiyama, T., Kamiya, T., Ban, Y., Ueda, Y., Kuse, Y. (2005). Test of Existing Low Concrete R/C Frame Strengthened with Concrete Member Included Steel Plate (Part 1) Ultimate Strength and Ductility of Beam and Column. *Summaries of technical papers of Annual Meeting Architectural Institute of Japan C-2: Structures IV*, 571-572., (in Japanese)
- [3] Sawazaki, E., Makitani, E., Uchida, M., Yoshioka, M., Suzuki, A. (2002). The experimental research on aseismic retrofit of the reinforced concrete column with low compressive strength. *Summaries of technical papers of Annual Meeting Architectural Institute of Japan C-2: Structures IV*, 377-378., (in Japanese)
- [4] Sawazaki, E., Makitani E., Tanigaki S., Ozone S. (2003). Experimental study on aseismic reinforcement of RC column with low compressive strength of concrete by Aramid continuous fiber sheets. *Summaries of technical papers of Annual Meeting Architectural Institute of Japan C-2: Structures IV*, 267-268., (in Japanese)
- [5] Aiba, T., Makitani, E., Kosugi K., Tanigaki M., KAMIO T. (2004). The research on earthquake strengthening of the reinforced concrete column with low compressive strength. *Summaries of technical papers of Annual Meeting Architectural Institute of Japan C-2: Structures IV*, 579-580., (in Japanese)
- [6] Nagasaka, T., LIN, J., Hasegawa, K., Tojo, M. (2004). Loading Capacity and Deformability of R/C Beams with Extremely Low Strength Concrete. *Proceedings of the Japan Concrete Institute Vol. 26: No. 2*, 361-366., (in Japanese)
- [7] Neguchi, M., Fujiwara, K., Takatsuki, Y., Minami, K. (2007). Shear Failure Behavior of RC Columns with Low Strength Concrete and Round Reinforcement, *Proceedings of the Japan Concrete Institute vol. 29: No.3*, 157-162., (in Japanese)
- [8] Neguchi, M., Kawakami, H., Takatsuki, Y., Minami, K. (2008). Shear Failure Behavior on RC Columns with Low Strength Concrete of 10 N/mm^2 Grade. *Proceedings of the Japan Concrete Institute vol. 30: No.3*, 1129-1134., (in Japanese)
- [9] Architectural Institute of Japan (1990). Design Guideline for Earthquake Resistant Reinforced Concrete Buildings Based on Ultimate Strength Concept, (in Japanese)
- [10] Wakabayashi, M., Minami, K. (1979). Some Tests on the Method to Prevent Shear Failure in Reinforced Concrete Columns. *Annals of Desaster Prevention Research Institute, Kyoto Univ. Vol. 22: B-1*, 295-316., (in Japanese)
- [11] Richart, F. E., Brandtzaeg, A. and Brown, R. L. (1929). The Failure of Plain and Spirally Reinforced Concrete in Compression. *Engineering Experiment Station*. University of Illinois Bulletin, Univ. of Illinois **Bulletin No. 190**